Data Repository Item for "Glacio-isostatic control on hypoxia in a high-latitude shelf basin"

Tom Jilbert*[1], Daniel J. Conley[2], Bo G. Gustafsson[3], Carolina P. Funkey[2], Caroline P. Slomp[1]

[1]Department of Earth Sciences (Geochemistry), Faculty of Geosciences, Utrecht University P.O. Box 80.021, 3508 TA Utrecht, The Netherlands

[2]Department of Geology, Lund University, Sölvegatan 12, S-223 62 Lund, Sweden

[3]Baltic Nest Institute, Baltic Sea Centre, Stockholm University, S-106 91 Stockholm, Sweden

**Corresponding author, now at: Department of Environmental Sciences, P.O. Box 65, 00014 University of Helsinki, Helsinki, Finland, tom.jilbert@helsinki.fi, Tel: +358919157923*

COMPLETE METHODS

Sediment coring, sampling and chemical analysis

Sediment multi-cores and gravity cores were collected from sites LL19 in the Baltic Proper (58.8807°N, 20.3108°E, 169m water depth) and SR5 in the Bothnian Sea (61.0833°N, 19.5797°E, 126m water depth) during cruises with R/V Aranda in May/June 2009 and R/V Skagerak in October 2008 (Fig. 1 of main article). All cores were sliced at 0.5-2 cm resolution in a nitrogen- or argon-filled glovebox. Sediment samples were freeze-dried and returned to the glovebox to be powdered and ground in an agate mortar. Subsamples were decalcified by shaking in excess 1M HCl, initially for 12 h and for a further 4 h after addition of new acid. The decalcified sediment was dried, ground in an agate mortar and analyzed by combustion for C_{org} by Fisons NA 1500 NCS (precision and accuracy <2% based on an atropine/acetanilide standard calibration and checked against internal laboratory standard sediments). A second subsample was dissolved in 2.5 ml HF (40 %) and 2.5 ml of an $HClO_4/HNO_3$ mixture, in a closed Teflon bomb at 90 °C for 12 h. The acids were then evaporated at 190 °C and the resulting gel was dissolved in 1M HNO_3, and analyzed for Mo (202.030 nm), P (177.495nm), and Al (308.215 nm) among other elements by ICP-OES (Ametek Spectro Arcos, precision and accuracy <5 %, based on calibration to standard solutions and checked against internal laboratory standard sediments). A parallel series of samples was taken at 1-5 cm resolution in a dark lab in preparation for pigment analysis. These samples were freeze-dried and ground, then mixed with cold HPLC-grade acetone: methanol: milliQ water (80:15:5%), sonicated and stored in a freezer (-20°C) overnight. Extracts were centrifuged and filtered at 0.45µm, and analyzed by high performance liquid chromatography (HPLC) on a Shimadzu Prominence HPLC equipped with an on-line photodiode array detector (SPD-M20A PDA) and an auto-sampler (Sil-10AF). See Funkey et

al. (2014) for more details. All raw elemental and pigment concentration data are presented in Table DR2.

Core chronologies

Multi-core and gravity core data were combined on the basis of overlaps in the geochemical profiles. LL19 has been comprehensively dated as described elsewhere (Jilbert and Slomp, 2013) by ^{210}Pb dating of the upper sediments and matching of the C_{org} profile of deeper sediments to Loss on Ignition (LOI) in the Pb pollution-isochrone/PSV-dated master core 372740-3 from the Gotland Deep (Lougheed et al., 2012a). This chronology was used to determine the duration of the hypoxic interval during the Holocene Thermal Maximum (HI_{HTM}) in the Baltic Proper, and the timing of its termination at ~4.0 ka (Fig. DR1). PSV dating is unavailable for SR5, and accurate radiocarbon dating of Baltic Sea sediments in general is hampered by reservoir age uncertainties and the potential for contamination with reworked carbon (Lougheed et al., 2012b). Therefore we focused on estimating the duration of the HI_{HTM} in the Bothnian Sea to assess the possibility of co-eval deposition with the HI_{HTM} in the Baltic Proper. Six bulk-sediment radiocarbon dates were obtained from core MSM-16/1-082-03 (61.0768°N, 20.6233°E) including 5 within the HI_{HTM} as determined by elevated C_{org} values. ^{14}C determinations were carried out at the Lund University Accelerator Mass Spectrometry (AMS) laboratory. MSM-16/1-082-03 is located very close to SR5 and shows a comparable C_{org} profile. Equivalent depths in MSM-16/1-082-03 and SR5 were thus identified by matching the C_{org} profiles of the two cores. The duration of the HI_{HTM} in SR5 was then estimated by calibrating the oldest and youngest radiocarbon dates of the HI_{HTM} to calendar ages using the Marine13 calibration curve in Oxcal v4.2 (Bronk Ramsey, 2009) (Fig. DR1). This calculation was performed assuming a reservoir age offset (ΔR) of 0 years and applying no correction for reworked carbon. Hence, the derived ages are expected to be older than the true ages of the sediments, potentially by >1000 years (Lougheed et al., 2012b). If

ΔR and the contribution of reworked carbon are assumed constant, the duration of the HI_{HTM} in the Bothnian Sea is estimated at ~3.8 k.y., which is in the same range as the 3.3 k.y. duration estimated for the HI_{HTM} in the Baltic Proper (Fig. DR1).

Bathymetric modelling

The bathymetric modelling is based on the empirical shore-level displacement model described in Påsse and Andersson (2005). These authors assumed isostatic uplift of Fennoscandia over the period 20 ka–present to be represented by a composite curve of one slow and one fast component, for which general mathematical expressions could be formulated. Taking into account eustatic sea level rise, the parameters of the expressions were fitted to empirical data on shore-level curves from 79 sites distributed across Scandinavia. We interpolated these parameters across a 2D grid of present day elevation in the Baltic region (2 by 1 minute in longitude and latitude, respectively, www.io-warnemuende.de/iowtopo). Past elevation at any position on the grid was calculated by subtracting uplift and eustatic sea level rise from the present day value. This simple means of calculation neglects possible bathymetric changes due to sediment accumulation and erosion. However, this is only relevant for deep basins areas, where accumulation is substantial, and not to the inter-basin sill areas, which are dominated by bedrock.

SUPPLEMENTARY FIGURES

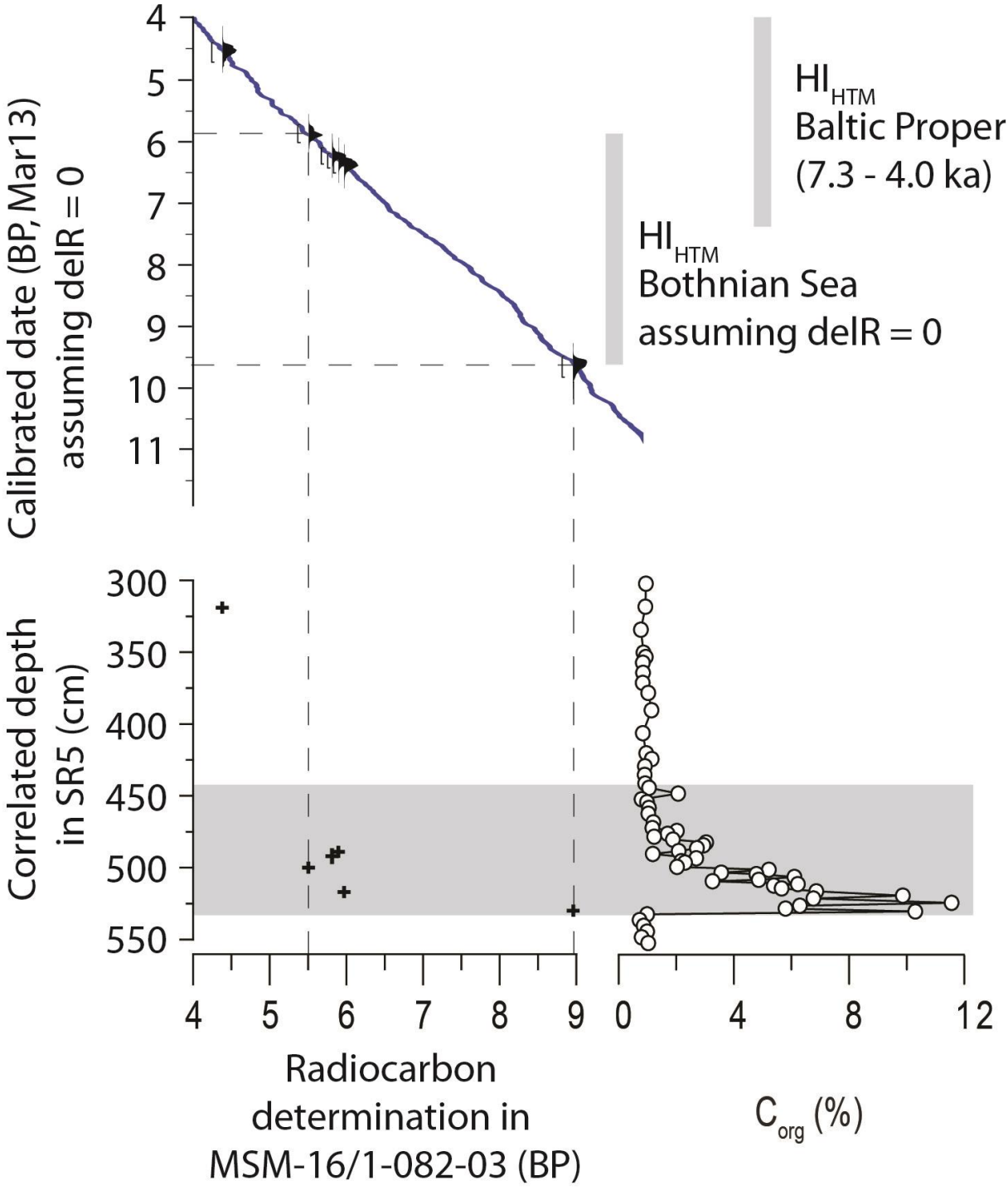

Figure DR1. Radiocarbon dating of Bothnian Sea sediments. Six bulk radiocarbon ages were determined in samples from core MSM-16/1-082-03. The equivalent depths of the six points in SR5 were determined by correlation of the C_{org} profiles of the two cores. Five of the points fall within the boundaries of the C_{org} excursion corresponding to the HI_{HTM} (indicated by the horizontal gray bar, 440-530 cm). Vertical dashed lines indicate the maximum radiocarbon age range of points within the HI_{HTM}. Calibration of this range to Marine13 (upper plot, assuming reservoir age offset (ΔR) = 0 and applying no correction for reworked carbon) yields a duration of the HI_{HTM} of ~3.8 k.y. The age and duration of the HI_{HTM} in the Baltic Proper (3.3 k.y. from 7.3 – 4.0 ka; Jilbert and Slomp, 2013) is shown for comparison. The HI_{HTM} in the Baltic Proper is dated by Paleomagnetic Secular Variation (PSV) and has an absolute age uncertainty of <0.5 k.y.

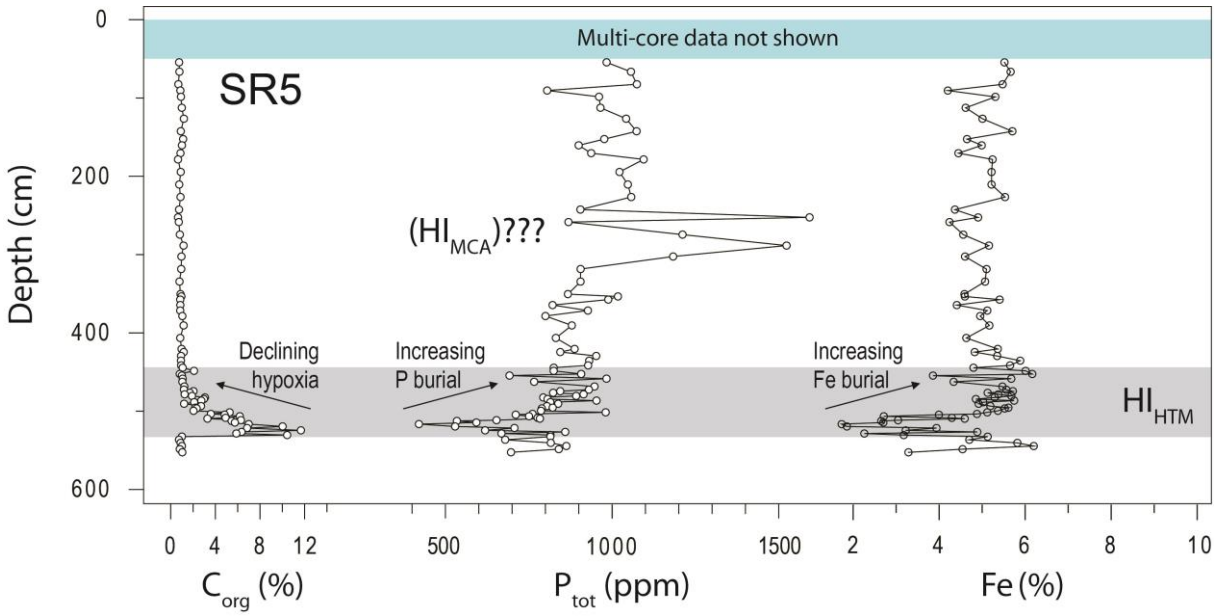

Figure DR2. C_{org}, P and Fe concentrations at SR5. The hypoxic interval during the Holocene Thermal Maximum (HI_{HTM}) is indicated by the horizontal gray bar. Multi-core data are not shown, in order to expand the scale on the P axis to highlight changes in the gravity core profile (extreme P concentrations in the surface sediments are related to modern-day cycling of P and are not representative for P concentrations upon burial).

SUPPLEMENTARY DISCUSSION

Changes in P burial rate in the Bothnian Sea

Assuming the termination of the HI_{HTM} (as determined by enhanced C_{org} values) at SR5 to occur at 4.0 ka, and the total duration of the HI_{HTM} at SR5 to be 3.8 k.y. (Fig. DR1), we calculated mean P burial rates for the HI_{HTM} and post-HI_{HTM} (i.e. 4.0 – present) intervals (Table DR1). These indicate a seven-fold higher mean P burial rate in the post-HI_{HTM} interval, the majority of the increase being caused by higher mass accumulation rates. However, mean P concentrations are also higher during the post-HI_{HTM} interval (Table DR1; Fig, DR2), suggesting a higher efficiency of P retention in Bothnian Sea sediments after the HI_{HTM}.

In the absence of high-resolution mass accumulation rate estimates it is difficult to accurately reconstruct P burial rates on shorter timescales. However, the depth profile of P concentration suggests that major changes in P burial may have occurred at SR5, both during and after the HI_{HTM}. The early part of the HI_{HTM} at SR5 is characterized by the lowest P content of the entire record (Fig. DR2), leading to an extremely high C_{org}/P_{tot} ratio (Fig. 3 of main article), indicative of efficient regeneration of P from the sediments under strongly reducing conditions. Hereafter, P concentrations first rise steeply, and then more steadily across the termination of the HI_{HTM} (Fig. DR2). The increase mirrors the decline in C_{org} concentration, and suggests that the P burial rate increased as hypoxia became less intense due to shoaling of the deep water exchange. Furthermore, a parallel increase in the Fe concentration (Fig. DR2) suggests that this excess P was buried primarily in association with Fe, either as Fe oxyhydroxide-bound P or vivianite, as observed in the Bothnian Sea today (Slomp et al., 2013).

Interestingly, strongly elevated P concentrations are observed at 250–350 cm depth in SR5 (Fig. DR2). We speculate that this interval may be co-eval with the HI_{MCA} in the Baltic Proper, and that the high P concentrations result from enhanced export of surface-water P across the straits of the Åland Sea, analagous to the situation during the modern hypoxic event (Savchuk, 2005). However, there is no way to confirm this theory until improved dating is available for the post-HI_{HTM} interval at SR5.

SUPPLEMENTARY DATA TABLES

Table DR1. Calculation of P burial rates at SR5. The depth and duration of the HI_{HTM} are estimated as described in Fig. DR1.

Period	Depth interval (cm)	Estimated duration (yr)	Mean sedimentation rate (cm/yr)	Mean dry bulk density (g/cm^3)	Mean mass accumulation rate ($g/cm^2/yr$)	Mean P_{tot} content (ppm)	Mean P_{tot} accumulation rate ($g/cm^2/yr$)
Post- HI_{HTM}	0-440	4000	0.110	0.399	0.044	1062	$4.56x10^{-5}$
HI_{HTM}	440-530	3800	0.024	0.379	0.009	808	$7.36x10^{-6}$

Table DR2. Raw sediment geochemical data used in Figure 3 of the main article. Note that some data in the figures are presented as ratios of the raw data in this table. Al data are also presented to allow readers to calculate Mo/Al (as used in other studies, e.g., Jilbert and Slomp, 2013). Depth scales represent combined multi-core and gravity core profiles. Blank cells = no data.

SR5

Bulk sediment elemental data					**Pigment data in µmol/g bulk sediment (note independent depth scale and C_{org} series from bulk elements)**			
Depth	C_{org}	P	Mo	Al	Depth	C_{org}	Ech.	Zeax.
cm	*%*	*ppm*	*ppm*	*%*	*cm*	*%*	*µmol/g*	*µmol/g*
0.25	2.6	2783	5	7.5	1.5	3.1	0.0014	0.0000
0.75	2.6	2802	6	7.5	4.5	3.1	0.0010	0.0000
1.25	2.7	2927	5	7.8	7.8	3.0	0.0008	0.0015
1.75	2.7	2875	6	7.4	10.5	2.7	0.0006	0.0013
2.50	2.7	2864	6	7.1	13.5	2.7	0.0009	0.0018
3.50	2.8	2397	4	5.8	16.5	2.6	0.0006	0.0011
4.50	2.7	2585	4	6.0	19.5	2.5	0.0006	0.0013
5.50	2.5	2212	4	7.8	22.5	2.4	0.0006	0.0012
6.50	2.4	1242	3	8.3	25.5	2.3	0.0005	0.0010
7.50	2.3	1096	3	7.9	28.5	2.0	0.0007	0.0013
8.50	2.4	1206	3	8.3	31.5	1.9	0.0005	0.0000
9.50	2.4	1564	3	7.7	34.5	1.8	0.0005	0.0009
10.50	2.3	2025	3	8.0	37.5	1.9	0.0005	0.0010
12.00	2.3	1777	3	8.1	40.5	1.8	0.0006	0.0011
14.00	2.3	1285	5	8.0	31.5	1.9	0.0004	0.0007
16.00	2.2	1166	5	8.1	41.5	2.1	0.0004	0.0008
18.00	2.1	1228	4	8.4	50.0	2.0	0.0004	0.0007
20.00	1.3	1208	4	8.7	58.5	2.1	0.0004	0.0007
22.00	1.9	1123	3	8.4	68.5	1.9	0.0004	0.0009
24.00	1.6	1120	3	8.6	88.5	1.9	0.0004	0.0007
Depth	C_{org}	P	Mo	Al	Depth	C_{org}	Ech.	Zeax.
cm	*%*	*ppm*	*ppm*	*%*	*cm*	*%*	*µmol/g*	*µmol/g*
54.5	0.8	983	<2	7.9	98.5	2.3	0.0004	0.0009
66.5	0.8	1057	<2	8.1	118.5	2.6	0.0005	0.0010

82.5	0.7	1074	<2	8.0	128.5	2.6	0.0004	0.0007
90.5	0.9	805	<2	5.9	148.5	2.5	0.0006	0.0008
98.5	0.9	961	<2	7.0	158.5	2.5	0.0005	0.0009
112.5	1.0	965	<2	6.7	178.5	2.5	0.0005	0.0008
126.5	1.2	1042	<2	7.0	188.5	2.5	0.0004	0.0007
142.5	0.9	1073	<2	8.1	208.5	2.3	0.0004	0.0008
152.5	1.1	976	<2	7.0	218.5	2.3		
160.5	1.0	900	<2	6.6	228.5	2.2	0.0004	0.0007
170.5	0.9	937	<2	6.6	238.5	2.3	0.0005	0.0008
178.5	0.7	1095	<2	7.8	248.5	2.6	0.0005	0.0008
194.5	0.9	1022	<2	7.4	258.5	2.3	0.0006	0.0009
210.5	0.8	1047	<2	7.7	268.5	2.2		
226.5	0.9	1057	<2	7.8	278.5	2.3	0.0004	0.0007
242.5	0.7	905	5	6.9	288.5	2.3	0.0005	0.0007
252.5	0.7	1593	7	6.3	308.5	2.4	0.0005	0.0008

Depth *cm*	C_{org} *%*	P *ppm*	Mo *ppm*	Al *%*	Depth *cm*	C_{org} *%*	Ech. *µmol/g*	Zeax. *µmol/g*
258.5	0.7	869	<2	6.3	318.5	2.3	0.0007	0.0009
274.5	0.8	1211	<2	6.7	338.5	2.7	0.0006	0.0008
288.5	1.1	1523	<2	7.3	348.5	3.0	0.0006	0.0009
302.5	1.0	1183	<2	6.6	354.0	2.8	0.0004	0.0007
318.5	0.9	905	<2	7.2	358.0	2.7	0.0010	0.0013
334.5	0.8	905	<2	7.6	365.0	2.7	0.0010	0.0012
350.5	0.9	867	<2	6.8	372.0	2.7	0.0011	0.0017
353.5	1.0	1017	<2	7.1	379.0	2.9	0.0008	0.0010
357.5	0.9	988	9	8.3	391.0	2.9	0.0009	0.0007
364.5	0.9	821	<2	6.7	407.0	2.6	0.0012	0.0010
371.5	0.9	927	6	7.5	421.0	3.2	0.0013	0.0015
378.5	1.0	800	9	6.4	425.0	3.5	0.0011	0.0010
390.5	1.2	879	10	7.2	430.0	3.5	0.0020	0.0022
406.5	0.9	831	<2	6.7	436.0	3.2	0.0012	0.0010
420.5	1.0	888	5	7.2	442.0	2.8	0.0008	0.0008
424.5	1.2	844	13	6.6	445.0	3.0	0.0014	0.0013
429.5	0.9	952	19	.78	449.0	4.7	0.0047	0.0159
435.5	0.9	931	24	7.3	453.0	2.8	0.0016	0.0020

Depth *cm*	C_{org} *%*	P *ppm*	Mo *ppm*	Al *%*	Depth *cm*	C_{org} *%*	Ech. *µmol/g*	Zeax. *µmol/g*
441.5	0.9	928	20	7.8	455.0		0.0486	0.1888
444.5	1.1	825	21	6.6	459.0	3.1	0.0015	0.0017
448.5	2.1	825	52	6.0	463.0	2.8	0.0020	0.0026
452.5	0.8	907	15	7.6	469.0	3.2	0.0021	0.0027
454.5	1.0	692	6	5.8	473.0	3.6	0.0008	0.0014

458.5	1.1	983	11	7.9	475.0	4.5	0.0043	0.0082
462.5	1.0	766	13	6.1	477.0	5.4	0.0122	0.0279
468.5	1.2	947	24	8.0	479.0	5.4	0.0087	0.0216
472.5	1.2	930	40	7.3	481.0	3.2	0.0037	0.0056
474.5	2.0	844	61	6.4	483.0	6.7	0.0124	0.0242
476.5	1.7	823	36	6.6	485.0	7.7	0.0219	0.0484
478.5	1.2	914	22	7.8	487.0	6.2	0.0175	0.0336
480.5	1.9	892	68	6.8	489.0	6.0	0.0092	0.0120
482.5	3.1	793	101	5.1	491.0	4.4	0.0063	0.0111
484.5	3.0	806	75	5.7	494.0	5.1	0.0101	0.0190
486.5	2.7	953	116	6.5	496.0	6.7	0.0168	0.0288
488.5	2.1	815	36	6.7	497.0	5.3	0.0130	0.0217
490.5	1.2	838	21	7.0	500.0	8.8	0.0285	0.0543
493.5	2.7	804	72	5.9	502.0	8.3	0.0236	0.0463
495.5	2.2	822	76	6.6	504.0	11.2	0.0303	0.0869
496.5	2.3	789	95	5.9	505.0	10.5	0.0243	0.0728

Depth *cm*	C_{org} *%*	P *ppm*	Mo *ppm*	Al *%*	Depth *cm*	C_{org} *%*	Ech. *µmol/g*	Zeax. *µmol/g*
499.5	2.0	787	105	6.1	507.0	13.2	0.1114	0.1314
501.5	5.3	981		5.2	509.0	15.3	0.0937	0.3126
503.5	3.6	761	174	5.0	510.0	11.8	0.0698	0.1498
504.5	4.8	711	181	4.0	512.0	12.4	0.0647	0.1569
506.5	6.2	751	189	3.0	513.0	11.1	0.0520	0.1434
508.5	4.9	776	206	4.2	515.0	11.7	0.0891	0.2032
509.5	3.3	783	142	5.0	516.0	12.8	0.1644	0.3043
511.5	6.3	653	120	3.5	519.0	16.0	0.1402	0.3188
512.5	5.5	534	118	2.7	521.0	18.3	0.3514	0.3870
514.5	5.7	593	156	2.6	524.0	14.7	0.1192	0.1535
516.5	7.0	420	128	1.7	526.0	15.5	0.1266	0.1976
519.5	10.0	529	177	1.9	529.0	17.8	0.1402	0.2942
521.5	6.8	707	250	3.1	531.0	17.1	0.1240	0.4814
524.5	11.7	619	188	2.9	533.0	9.4	0.0281	0.1323
526.5	6.4	859	237	4.3	537.0	2.0	0.0004	0.0008
528.5	5.9	668	190	2.3	540.0	2.5	0.0000	0.0021
530.5	10.4	815	240	3.4	544.0	2.5	0.0004	0.0008
532.5	1.0	815	30	6.3	548.0	2.3	0.0004	0.0009
536.5	0.7	679	11	6.1	553.0	3.0	0.0003	0.0008

Depth *cm*	C_{org} *%*	P *ppm*	Mo *ppm*	Al *%*	Depth *cm*	C_{org} *%*	Ech. *µmol/g*	Zeax. *µmol/g*
540.5	0.9	816	13	6.9				
544.5	1.0	863	12	7.2				

548.5	0.8	840	<2	6.7
552.5	1.0	697	<2	5.6

LL19

Bulk sediment elemental data					**Pigment data in µmol/g bulk sediment (note independent depth scale and C_{org} series from bulk elements)**			
Depth	C_{org}	P	Mo	Al	Depth	C_{org}	Ech.	Zeax.
cm	*%*	*ppm*	*ppm*	*%*	*cm*	*%*	*µmol/g*	*µmol/g*
0.25	11.83	1709	155	5.3	5.5	9.72	0.0133	0.0466
0.75	13.65	1794	216	5.1	7.5	8.38	0.0099	0.0375
1.25	12.87	1709	206	5.2	9.5	2.79	0.0009	0.0026
1.75	11.68	1570	196	5.6	11.5	2.46	0.0015	0.0030
2.50	9.82	1345	159	6.1	13.5	2.15	0.0013	0.0025
3.50	8.83	1284	160	6.4	15.5	2.10	0.0010	0.0019
4.50	8.44	1252	167	6.3	17.5	2.10	0.0010	0.0025
5.50	8.47	1370	160	6.1	19.5	2.01	0.0010	0.0020
6.50	7.59	1277	181	6.3	21.5	2.00	0.0011	0.0022
7.50	7.73	1194	221	6.4	23.5	1.97	0.0010	0.0019
8.50	7.18	1056	122	5.9	25.5	2.02	0.0011	0.0019
9.50	3.74	961	24	7.6	27.5	2.08	0.0010	0.0020
11.00	2.87	872	11	8.7	29.5	2.16	0.0011	0.0020
13.00	2.48	849	11	8.8	31.5	2.23	0.0011	0.0020
15.00	2.21	860	11	9.1	33.5	2.27	0.0011	0.0019
17.00	1.42	795	8	8.6	35.5	2.25	0.0012	0.0020
19.00	1.88	775	8	8.3	37.5	2.25	0.0006	0.0013
21.00	1.83	791	6	8.7	39.5	2.13	0.0011	0.0021
23.00	1.57	816	5	8.9	41.5	2.10	0.0010	0.0019
25.00	1.96	838	5	8.9	43.5	2.11	0.0010	0.0017
27.00	2.08	821	<2	8.4	45.5	2.15	0.0009	0.0016

Depth	C_{org}	P	Mo	Al	Depth	C_{org}	Ech.	Zeax.
cm	*%*	*ppm*	*ppm*	*%*	*cm*	*%*	*µmol/g*	*µmol/g*
29.00	2.01	804	5	8.4	68.5	2.5	0.0004	0.0005
31.00	1.99	856	7	8.8	70.5	2.6	0.0005	0.0005
33.00	1.92	821	9	8.5	72.5	2.5	0.0005	0.0008
35.00	1.80	786	8	8.1	74.5	2.7	0.0008	0.0022
37.00	1.84	825	11	8.5	76.5	3.0	0.0007	0.0013
39.00	2.01	846	8	8.7	77.5	3.0	0.0007	0.0011
41.00	1.88	837	17	8.8	79.5	3.2	0.0011	0.0022
43.00	1.93	764	5	8.3	81.5	2.9	0.0015	0.0044

45.00	1.93	819	8	8.7	83.5	3.0	0.0011	0.0037
47.00	1.94	841	14	8.9	86.5	3.0	0.0015	0.0031
49.00	1.85	793	13	8.5	88.5	4.3	0.0040	0.0200
51.00	1.92	750	6	8.2	90.5	8.4	0.0195	0.0754
53.00	1.95	777	8	8.3	92.5	7.5	0.0153	0.0639
55.00	2.00	777	12	8.0	94.5	6.8	0.0117	0.0434
56.50	2.03	834	20	8.6	96.5	5.8	0.0089	0.0385
57.50	2.17	789	24	7.9	98.5	3.5	0.0033	0.0118
58.50	2.15	762	28	7.9	100.5	3.3	0.0039	0.0169

Depth *cm*	C_{org} *%*	P *ppm*	Mo *ppm*	Al *%*	Depth *cm*	C_{org} *%*	Ech. *µmol/g*	Zeax. *µmol/g*
59.50	2.26	800	30	8-4	102.5	4.9	0.0082	0.0353
60.50	2.19	825	18	8.6	104.5	3.8	0.0040	0.0158
61.50	2.20	842	20	8.7	106.5	3.4	0.0037	0.0153
62.50	2.15	784	22	8.1	109.5	2.2	0.0012	0.0034
63.50	2.21	728	15	7.7	124.0	2.2	0.0012	0.0010
64.50	2.18	800	23	8.2	144.0	1.8	0.0007	0.0012
65.50	2.08	746	13	7.9	164.0	1.9	0.0007	0.0011
66.50	2.17	699	12	7.1	174.0	2.0	0.0010	0.0029
67.50	2.07	752	23	7.2	184.0	2.0	0.0009	0.0016
68.50	2.23	694	13	7.2	204.0	1.9	0.0006	0.0009
69.50	2.22	710	14	7.5	214.0	2.1	0.0018	0.0013
70.50	2.37	785	19	8.0	224.0	2.0	0.0012	0.0024
71.50	2.19	781	13	8.1	234.0	1.9	0.0007	0.0007
72.50	2.31	734	10	7.6	244.0	2.0	0.0013	0.0031
73.50	2.11	816	17	8.0	254.0	2.2	0.0021	0.0070
74.50	2.21	998	12	7.2	262.0	2.1	0.0026	0.0071
75.50	2.14	840	<2	6.7	265.5	2.3	0.0013	0.0034
77.00	2.31	706	<2	6.1	266.5	2.1	0.0010	0.0014
79.00	2.52	638	20	6.1	267.5	2.3	0.0012	0.0023

Depth *cm*	C_{org} *%*	P *ppm*	Mo *ppm*	Al *%*	Depth *cm*	C_{org} *%*	Ech. *µmol/g*	Zeax. *µmol/g*
81.00	2.37	648	20	6.4	268.5	2.5	0.0015	0.0029
83.00	2.33	737	18	6.7	270.5	4.0	0.0050	0.0203
85.00	2.52	848	17	8.7	272.5	4.5	0.0037	0.0169
86.50	2.71	879	23	8.7	274.5	5.0	0.0064	0.0314
87.50	2.79	875	23	8.6	276.5	8.0	0.0107	0.0458
88.50	3.46	865	28	8.2	278.5	7.9	0.0200	0.0700
89.50	4.93	938	124	8.0	280.5	5.3	0.0104	0.0383
90.50	7.49	928	254	6.5	282.5	3.5	0.0033	0.0166
91.50	6.57	936	245	6.6	284.5	5.8	0.0056	0.0245
92.50	5.15	886	135	7.2	286.5	5.3	0.0063	0.0237

93.50	5.30	894	112	7.3	288.5	3.8	0.0032	0.0126
94.50	4.29	1025	79	9.2	290.5	6.1	0.0068	0.0291
95.50	4.73	857	52	7.2	292.5	6.2	0.0120	0.0319
96.50	4.37	813	59	6.9	294.5	3.8	0.0041	0.0121
97.50	3.00				296.5	2.0	0.0011	0.0020
98.50	3.37				298.5	1.7	0.0005	0.0005
99.50	3.33	889	15	8.0	300.5	2.2	0.0010	0.0007
100.50	3.21	838	16	8.0	302.5	4.4	0.0083	0.0200
101.50	3.48	885	16	8.6	304.5	2.1	0.0018	0.0021

Depth *cm*	C_{org} *%*	P *ppm*	Mo *ppm*	Al *%*	Depth *cm*	C_{org} *%*	Ech. *µmol/g*	Zeax. *µmol/g*
102.50	3.68	838	17	7.7	306.5	2.2	0.0016	0.0020
103.50	3.41	867	20	7.6	308.5	3.3	0.0068	0.0131
104.50	3.93	793	29	7.1	310.5	3.0	0.0036	0.0052
105.50	3.71	836	25	7.9	312.5	10.3	0.0399	0.0994
106.50	3.16	753	17	7.3	314.5	2.6	0.0005	0.0005
107.50	3.03	860	17	8.4	316.5	1.9	0.0004	0.0000
108.50	2.40	810	8	8.5	318.5	2.4	0.0008	0.0012
109.50	2.08	799	6	8.8	320.5	3.0	0.0016	0.0026
110.50	1.98	765	7	8.4	322.5	3.3	0.0009	0.0019
122.00	1.76	780	5	8.6	326.5	3.3	0.0009	0.0021
134.00	2.11	781	6	8.4	328.5	3.2	0.0005	0.0008
146.00	2.23	800	10	8.5	329.5	3.4	0.0005	0.0015
158.00	1.74	773	6	8.8	331.5	2.8	0.0004	0.0013
170.00	1.82	739	<2	8.3	333.5	2.4	0.0004	0.0009
182.00	1.87	808	4	8.9	335.5	2.3	0.0003	0.0005
194.00	2.11	806	8	9.0	337.5	1.9	0.0004	0.0005
204.00	1.86	789	4	8.8	339.5	1.6	0.0003	0.0000

Depth *cm*	C_{org} *%*	P *ppm*	Mo *ppm*	Al *%*	Depth *cm*	C_{org} *%*	Ech. *µmol/g*	Zeax. *µmol/g*
216.00	1.80	842	7	9.2	342.5	1.0	0.0000	0.0000
228.00	1.73	735	2	8.4	343.5	1.2	0.0000	0.0000
240.00	1.63	777	4	8.9	345.5	1.2	0.0000	0.0000
242.00	1.67	713	3	8.2	347.5	1.1	0.0000	0.0000
244.00	1.78	807	4	9.2	349.5	0.9	0.0000	0.0000
246.00	1.75	777	6	8.9	354.5	1.1	0.0000	0.0000
248.00	1.83	823	4	9.2	355.5	1.1	0.0000	0.0005
250.00	1.82	822	5	9.2	357.5	1.0	0.0000	0.0005
252.00	1.97	640	6	7.3	359.5	1.0	0.0000	0.0000
254.00	2.30	743	7	8.1	361.5	1.0	0.0000	0.0005
256.00	1.87	809	6	9.1	363.5	1.0	0.0000	0.0000
258.00	2.10	796	7	8.5	366.5	0.8	0.0000	0.0004

260.00	1.94	779	6	8.9	367.5	0.9	0.0000	0.0000
262.00	1.94	811	8	8.6	374.0	0.9	0.0000	0.0000
264.00	2.01	733	9	8.0	384.0	0.8	0.0000	0.0004
265.50	2.11	812	10	8.7	394.0	0.5	0.0000	0.0004
266.50	1.89	818	7	8.9				
267.50	2.00	807	6	8.8				
268.50		820	9	8.8				

Depth	C_{org}	P	Mo	Al
cm	*%*	*ppm*	*ppm*	*%*
269.50	2.93	784	15	8.1
270.50	3.16	820	26	8.2
271.50	3.37	791	22	8.0
272.50	3.51	848	32	8.1
273.50	4.77	832	115	7.3
274.50	4.30	1028	71	7.9
275.50	6.67	904	205	7.0
276.50	5.88	853	152	7.1
277.50	7.91	849	246	6.4
278.50	6.41	868	224	7.0
279.50	5.09	839	160	7.7
280.50	4.94	779	103	7.2
281.50	4.22	854	44	8.1
282.50	3.43	833	40	8.1
283.50	3.69	768	29	7.9
284.50	4.68	774	72	7.1
285.50	4.85	795	81	7.4
286.50	3.94	847	35	8.4

Depth	C_{org}	P	Mo	Al
cm	*%*	*ppm*	*ppm*	*%*
287.50	4.59	829	76	7.7
288.50	3.61	678	35	7.1
289.50	3.21	776	24	8.1
290.50	4.84	793	66	7.4
291.50	4.44	749	63	7.2
292.50	5.41	802	99	7.3
293.50	4.58	789	61	7.9
294.50	2.74	800	33	8.6
295.50	1.75	664	5	8.0
296.50	1.90	683	7	7.9
297.50	1.67	727	11	7.7
298.50	1.57	740	15	8.3
299.50	1.73	843	12	9.1

300.50	2.06	781	15	9.0
301.50	2.52	744	24	8.4
302.50	3.82	828	48	8.4
303.50	2.48	810	19	8.3
304.50	2.10	742	14	8.5

Depth	C_{org}	P	Mo	Al
cm	*%*	*ppm*	*ppm*	*%*
305.50	2.15	753	12	8.4
306.50	1.98	746	17	8.5
307.50	2.39	772	18	8.5
308.50	3.28	788	35	8.1
309.50	2.43	788	32	8.5
310.50	5.03	790	99	7.4
311.50	8.02	874	237	6.8
312.50	8.36	858	267	6.6
313.50	6.54	887	212	7.0
314.50	1.77	809	26	7.6
315.50	1.75	897	32	8.3
316.50	1.81	779	16	8.5
317.50	1.95	764	16	8.6
318.50	1.94	784	32	7.6
319.50	2.50	829	14	8.8
320.50	3.19	796	16	8.3
321.50	3.71	772	24	8.0
322.50	2.69	797	23	8.6
323.50	3.33	818	20	7.9

Depth	C_{org}	P	Mo	Al
cm	*%*	*ppm*	*ppm*	*%*
324.50	2.76	936	19	8.2
325.50	2.84	925	28	7.9
327.00	2.55	824	35	8.3
329.00	2.70	766	39	7.6
331.00	2.35	795	17	7.7
333.00	2.07	824	10	8.9
337.00	1.92	816	4	9.0
339.00	1.40	736	<2	9.1
343.00	0.90	547	<2	7.7
345.00		652	<2	9.2
349.00	0.88	659	<2	9.2
353.00	0.82	672	<2	9.3
355.00	0.99	592	<2	8.5
357.00	0.88	674	<2	9.5

361.00	0.88	645	<2	9.1
365.00	0.73	667	2	9.6
367.00	0.91	639	<2	9.3
369.00	0.52	653	2	9.1

Depth	C_{org}	P	Mo	Al
cm	*%*	*ppm*	*ppm*	*%*
373.00	1.09	667	<2	9.2
377.00	0.66	669	<2	9.3
379.00		645	<2	9.0
381.00	0.65	727	<2	9.9
385.00	0.57	710	<2	9.5
389.00	0.43	708	2	9.5
391.00	0.55	676	<2	9.2
393.00	0.52	700	2	9.6
397.50	0.53	763	2	10.1

SUPPLEMENTARY REFERENCES

Bronk Ramsey, C. B., 2009, Bayesian Analysis of Radiocarbon Dates: Radiocarbon, v. 51, no. 1, p. 337–360.

Funkey, C. P., Conley, D. J., Reuss, N. S., Humborg, C., Jilbert, T., and Slomp, C. P., 2014, Hypoxia sustains cyanobacteria blooms in the Baltic Sea: Environmental Science & Technology, v. 48, no. 5, p. 2598–2602.

Jilbert, T. and Slomp, C.P., 2013, Rapid high-amplitude variability in Baltic Sea hypoxia during the Holocene: Geology, v. 41, p. 1183–1186.

Lougheed, B.C., Snowball, I., Moros, M., Kabel, K., Muscheler, R., Virtasalo, J.J., and Wacker, L., 2012a, Using an independent geochronology based on palaeomagnetic secular variation (PSV) and atmospheric Pb deposition to date Baltic Sea sediments and infer C-14 reservoir age: Quaternary Science Reviews, v. 42, p. 43–58.

Lougheed, B.C., Filipsson, H.L. and Snowball, I., 2012b, Large spatial variations in coastal C-14 reservoir age: A case study from the Baltic Sea. Climate of the Past, v. 9, p. 1015–1028.

Påsse, T. and Andersson, L., 2005, Shore-level displacement in Fennoscandia calculated from empirical data. GFF, v. 127, p. 253–268.

Savchuk, O.P., 2005, Resolving the Baltic Sea into seven subbasins: N and P budgets for 1991–1999: Journal of Marine Systems, v. 56, no. 1–2, p. 1–15.

Slomp, C.P., Mort, H.P., Jilbert, T., Reed, D.C., Gustafsson, B.G., and Wolthers, M., 2013, Coupled dynamics of iron and phosphorus in sediments of an oligotrophic coastal basin and the impact of anaerobic oxidation of methane: PLoS ONE, v. 8, no. 4, p. e62386.